

1 **A Comparison of Variational, Differential Quadrature and**
2 **Approximate Closed Form Solution Methods for Buckling**
3 **of Highly Flexurally Anisotropic Laminates**

4 Zhangming Wu ¹ and Gangadharan Raju ², and Paul M Weaver ³,

5 **ABSTRACT**

6 The buckling response of symmetric laminates that possess strong flexural-twist
7 coupling are studied using different methodologies. Such plates are difficult to analyse
8 due to localised gradients in the mode shape. Initially, the energy method (Rayleigh-
9 Ritz) using Legendre polynomials is employed and the difficulty of achieving reliable
10 solutions for some extreme cases is discussed. To overcome the convergence problems,
11 the concept of Lagrangian multiplier is introduced into the Rayleigh-Ritz formulation.
12 The Lagrangian multiplier approach is able to provide the upper and lower bounds of
13 critical buckling load results. In addition, mixed variational principles are used to gain a
14 better understanding of the mechanics behind the strong flexural-twist anisotropy effect
15 on buckling solutions. Specifically, the Hellinger-Reissner variational principle is used to
16 study the effect of flexural-twist coupling on buckling and also to explore the potential

¹Research Assistant, ACCIS, Dept. of Aerospace Engineering, Univ. of Bristol, Queen's Building, Bristol BS8 1TR, U.K.

²Research Assistant, ACCIS, Dept. of Aerospace Engineering, Univ. of Bristol, Queen's Building, Bristol BS8 1TR, U.K.

³Professor in Lightweight Structures, ACCIS, Dept. of Aerospace Engineering, Univ. of Bristol, Queen's Building, Bristol BS8 1TR, U.K. (corresponding author) E-mail: Paul.Weaver@bristol.ac.uk

17 for developing closed form solutions for these problems. Finally, solutions using the
18 differential quadrature method are obtained. Numerical results of buckling coefficients
19 for highly anisotropic plates with different boundary conditions are studied using the
20 proposed approaches and compared with finite element results. The advantages of both
21 Lagrangian multiplier theory and variational principle in evaluating buckling loads are
22 discussed. In addition, a new simple closed form solution is shown for the case of a
23 flexurally anisotropic plate with three sides simply supported and one long edge free.
24 **Keywords:** Buckling, Flexural-twist coupling, Lagrangian Multiplier, Hellinger-
25 Reissner variational principle, Differential Quadrature Method

26 INTRODUCTION

27 Laminated composite structures provide structural engineers with extended
28 design space and tailorability options which helps facilitate the design of efficient,
29 lightweight structures. Most laminated structures are designed to be balanced and
30 symmetric with angle plies such that the coupling between in-plane extension,
31 contraction with shear is avoided and any combination of these with bending or
32 twisting is also avoided yet still exhibit flexural-twist coupling to various degrees.
33 But, in the case of highly anisotropic composite plates, the effect of flexural-twist
34 coupling may be significant in the numerical evaluation of critical buckling load.
35 Therefore, a numerical methodology has to be developed for buckling analysis
36 of highly anisotropic composite structures. Earlier works of buckling analysis
37 on anisotropic plates were reported on the study of plywood plates (Balabuch
38 1937; Thielemann 1950; Green and Hearmon 1945). Green and Hearmon (Green
39 and Hearmon 1945) derived the formulation for buckling analysis of anisotropic
40 plates using Fourier series expansions, and also explored approximate closed-
41 form solutions of buckling load for infinite long anisotropic plate. Ashton and
42 Waddoups (Ashton and Waddoups 1969; Ashton 1969) applied the Rayleigh-Ritz

43 (RR) method to perform stability and dynamics analysis of anisotropic plates
44 with various boundary conditions. Later, Whitney (Whitney 1972) employed
45 the Fourier series approach proposed by Green to solve the vibration problem of
46 anisotropic plates with clamped edges. Chamis (Chamis 1969) used Galerkin's
47 method to perform the buckling analysis of anisotropic plates and concluded that
48 neglecting flexural-twist anisotropy could lead to non conservative buckling loads.

49 Nemeth (Nemeth 1986) defined the nondimensional parameters associated
50 with flexural-twist anisotropy and analysed the effects of flexural-twist anisotropy
51 on buckling of symmetric laminates. Tang *et al.* (Tang and Sridharan 1990)
52 and Grenestedt (Grenestedt 1989) employed a perturbation technique to study
53 the effect of flexural-twist anisotropy on buckling strength. Weaver (Weaver
54 2006) developed approximate closed-form (CF) expressions to study the effect of
55 flexural-twist anisotropy on buckling load of long anisotropic plates with simply-
56 supported sides subject to compression. Weaver and Nemeth (Weaver and Nemeth
57 2007) derived the bounds for non dimensional parameters governing the buckling
58 of anisotropic plates and this study provided insight into composite tailoring for
59 improving buckling resistance. Herencia *et al.* (Herencia et al. 2010) obtained
60 closed form solutions for buckling of long plates with flexural-twist anisotropy
61 with the short edges simply supported and with the longitudinal edges simply
62 supported, clamped, or elastically restrained in rotation under axial compression.
63 All of the above approaches give accurate results when applied to plates with low
64 to moderate flexural-twist anisotropy under different boundary conditions. How-
65 ever, when applied to laminates with extremely highly flexural-twist anisotropy,
66 they suffer from the issues of either very slow convergence or inaccurate results.

67 Initially, the RR method was applied to study the above problem using dif-
68 ferent orthogonal polynomials as admissible functions of plate deflection. Many
69 works have been reported in literature (Bhat 1985; Smith et al. 1999; Pandey

70 and Sherbourne 1991; Liew and Wang 1995; Chow et al. 1992) using orthogonal
71 polynomials in RR method for structural analysis. The results obtained using
72 orthogonal polynomials show better convergence when compared to Fourier se-
73 ries or beam mode shape functions. The reason is that, non-periodic polynomial
74 functions are better equipped than periodic trigonometric functions to capture
75 localised features, such as strong gradients in the buckling mode shape. In the
76 present work, Legendre polynomials were chosen as test functions to solve the
77 composite plate buckling problem and study the effect of bending-twisting cou-
78 pling coefficients(D_{16} and D_{26}) on buckling solutions(Nemeth 1986). The method
79 was not able to capture accurate buckling load results for some extreme cases,
80 such as the $[+45]_n$ all simply supported laminates and the $[+30]_n$ one edge free
81 laminates. The reason can be attributed to the non-satisfaction of natural bound-
82 ary conditions term by term which results in the slow convergence of the RR
83 method. In addition, the decreased accuracy of differentiation on the obtained
84 approximate deflection function will cause further errors in evaluation of moments
85 and forces.

86 In order to overcome convergence problems and improve the buckling results,
87 methodologies based on Lagrangian multipliers, Hellinger-Reissner (H-R) varia-
88 tional principle (Reissner 1950) and differential quadrature method (DQM) (Bell-
89 man 1971) are considered in this work. Following Budiansky and Hu's approach
90 (Budiansky and Hu 1946), the Lagrangian multiplier method using Legendre
91 polynomials is extended to study our test problems. The upper and lower bounds
92 of the solution can be obtained by varying the number of Lagrangian multiplier
93 terms and this concept is used for the evaluation of buckling load. In the approach
94 based on the H-R principle, the deflection and moments are allowed to vary inde-
95 pendently(Plass et al. 1962), while the relation between moments and deflection
96 (curvature) are weakly constrained in the defined functional. The constraints in

97 the functional between the different variables (functions) can be considered as
98 the method of Lagrangian multipliers(Chien 1984). In the current work, the de-
99 flection and moments are represented independently using Legendre polynomials
100 and the chosen polynomials satisfy the boundary conditions in terms of deflection
101 (w) and moments (M_x, M_y, M_{xy}). This approach is then applied to our test prob-
102 lems and the convergence of the buckling load results is studied. Furthermore,
103 as an alternative methodology to energy methods, DQM is also employed. DQM
104 is based on the quadrature method to approximate the derivatives of a function
105 and can be applied directly to solve the differential equation with appropriate
106 boundary conditions. Sherbourne *et al* (Sherbourne and Pandey 1991) studied
107 the accuracy and convergence of DQM for buckling analysis of anisotropic com-
108 posite plates under linearly varying compression load. Darvizeh *et al* (Darvizeh
109 et al. 2004) compared the performance of DQM with the RR method for buckling
110 analysis of composite plates. Herein, the buckling analysis of highly anisotropic
111 laminates is studied using DQM and the accuracy of the results are compared
112 with the other proposed approaches.

113 Thus the motivation of the present work is: (i) to develop robust and general-
114 ized methodologies for the buckling analysis of symmetric laminates with strong
115 flexural-twisting coupling, (ii) to study the effects of flexural-twist anisotropy on
116 buckling of long and short flexurally anisotropic plates under two sets of bound-
117 ary conditions using the proposed approaches and validate the results using finite
118 element method. Finally, a new approximate closed form solution is also offered
119 to provide a lower bound estimate for the buckling load of a long, flexurally
120 anisotropic plate with three sides simply supported and one long side free.

121 **FLEXURALLY ANISOTROPIC PLATE**

122 **Flexurally anisotropic plate formulation**

123 For a symmetrically laminated anisotropic plate subjected to uniaxial com-
 124 pression loading, the plate buckling behavior is governed by

$$\begin{aligned}
 & D_{11} \frac{\partial^4 w}{\partial x^4} + 2(D_{12} + 2D_{66}) \frac{\partial^4 w}{\partial x^2 \partial y^2} + D_{22} \frac{\partial^4 w}{\partial y^4} \\
 & + 4D_{16} \frac{\partial^4 w}{\partial x^3 \partial y} + 4D_{26} \frac{\partial^4 w}{\partial x \partial y^3} = N_x \frac{\partial^2 w}{\partial x^2}
 \end{aligned} \tag{1}$$

126 where D_{ij} ($i, j = 1, 2, 6$) and w are bending stiffness and out-of-plane deflection
 127 function of plate, respectively. The following four non-dimensional parameters of
 128 bending stiffness developed by Nemeth(Nemeth 1986),

$$\alpha = \sqrt[4]{\frac{D_{11}}{D_{22}}}; \beta = \frac{(D_{12} + 2D_{66})}{\sqrt{D_{11}D_{22}}}; \gamma = \frac{D_{16}}{\sqrt[4]{D_{11}^3 D_{22}}}; \delta = \frac{D_{26}}{\sqrt[4]{D_{22}^3 D_{11}}} \tag{2}$$

130 reflect the effects of orthotropy (α, β) and flexural-twist anisotropy (γ, δ) on plate
 131 buckling response. The bounds of these parameters were found to be $\alpha > 0$,
 132 $-1 < \beta < 3$, $|\gamma, \delta| < 1$ (Weaver and Nemeth 2007). When the absolute values of
 133 γ or δ are large, the plate is highly anisotropic and it may cause difficulties in the
 134 evaluation of its buckling load. In this paper, anisotropic plates with two different
 135 boundary conditions (Fig. 1) are considered, all simply-supported (SSSS) and one
 136 free edge and others simply-supported (SSSF).

137 **RAYLEIGH-RITZ FORMULATION**

138 The total potential energy of a plate under uniaxial compression is expressed
 139 as (Ashton and Waddoups 1969)

$$\Pi = U_b + \lambda U_T = \text{stationary value} \tag{3}$$

141 where U_b is the strain energy of plate, U_T is potential energy due to in-plane loads

142 and λ is the unknown buckling load proportionality factor. The potential energy
 143 can be expressed in the following convenient form with respect to normalised
 144 coordinates,

$$145 \quad \tilde{U}_b = \int_{-1}^1 \int_{-1}^1 \left[D_{11} \left(\frac{\partial^2 w}{\partial \xi^2} \right)^2 + 2\rho^2 D_{12} \frac{\partial^2 w}{\partial \xi^2} \frac{\partial^2 w}{\partial \eta^2} + \rho^4 D_{22} \left(\frac{\partial^2 w}{\partial \eta^2} \right)^2 \right. \\ \left. + 4\rho^2 D_{66} \left(\frac{\partial^2 w}{\partial \xi \partial \eta} \right)^2 + 2\rho D_{16} \frac{\partial^2 w}{\partial \xi^2} \frac{\partial^2 w}{\partial \xi \partial \eta} + 2\rho^3 D_{26} \frac{\partial^2 w}{\partial \eta^2} \frac{\partial^2 w}{\partial \xi \partial \eta} \right] d\xi d\eta \quad (4)$$

$$146 \quad \tilde{U}_T = \int_{-1}^1 \int_{-1}^1 N_x \left(\frac{\partial w}{\partial \xi} \right)^2 d\xi d\eta \quad (5)$$

147 where $\rho = a/b$ is the aspect ratio and a, b are the length and width of the plate,
 148 respectively. The nondimensional parameters ξ, η are defined as $\xi = 2x/a, \eta =$
 149 $2y/b$ ($\xi, \eta \in [-1, 1]$). The out-of-plane deflection of plate is assumed to be of the
 150 form,

$$151 \quad w(\xi, \eta) = \sum_{m=1}^M \sum_{n=1}^N A_{mn} X_m(\xi) Y_n(\eta) \quad (6)$$

152 where A_{mn} are the unknown deflection coefficients, $X_m(x)$ and $Y_n(y)$ are admissi-
 153 ble functions satisfying the geometry boundary conditions. The numbers M and
 154 N denote the number of admissible functions $X_m(x)$ and $Y_n(y)$ employed in RR
 155 method, respectively. In this work Legendre polynomials are chosen for analysis
 156 due to superior convergence properties in capturing localised features, defined as,

$$P_1 = 1, \quad P_2 = \xi, \quad P_3 = \frac{1}{2}(3\xi^2 - 1) \dots \\ 157 \quad P_{i+1}(\xi) = \sum_{j=0}^i (-1)^j \frac{(2i-2j)!}{2^i j! (i-j)! (i-2j)!} \xi^{i-2j} \quad (7) \\ j = \frac{i}{2} (i = 0, 2, 4, \dots), \quad \frac{i-1}{2} (i = 1, 3, 5, \dots)$$

158 The admissible functions when applied to the above mentioned plate boundary
 159 conditions can be written in the following form,

$$\begin{aligned}
 X_m(\xi) &= (1 - \xi)^\iota (1 + \xi)^\iota P_m(\xi) \\
 Y_n(\eta) &= (1 - \eta)^\iota (1 + \eta)^\iota P_n(\eta)
 \end{aligned}
 \tag{8}$$

161 where $\iota = 0, 1, 2$ for the boundary conditions of free, simply-supported and
 162 clamped edges, respectively. The total potential energy Π is then minimised
 163 with respect to A_{mn} and the resulting matrix expression is given as,

$$\{\mathbf{K} + \lambda\mathbf{L}\} \{\mathbf{A}\} = 0
 \tag{9}$$

165 where $[\mathbf{A}] = [A_{11}, A_{12} \dots, A_{MN}]^T$. The elements of matrix \mathbf{K} and \mathbf{L} are given as
 166 follows,

$$\begin{aligned}
K_{ij} &= U_{b,mnrs} = \\
&\int_{-1}^1 \int_{-1}^1 \left[D_{11} X_{m,\xi\xi} Y_n X_{r,\xi\xi} Y_s \right. \\
&+ \rho^2 D_{12} (X_m Y_{n,\eta\eta} X_{r,\xi\xi} Y_s + X_{m,\xi\xi} Y_n X_r Y_{s,\eta\eta}) \\
&+ \rho^4 D_{22} X_{m,\xi\xi} Y_n X_{r,\xi\xi} Y_s + \rho^2 D_{66} X_{m,\xi} Y_{n,\eta} X_{r,\xi} Y_{s,\eta} \\
&+ \rho D_{16} (X_{m,\xi} Y_{n,\eta} X_r Y_{s,\eta\eta} + X_m Y_{n,\eta\eta} X_{r,\xi} Y_{s,\eta\eta}) \\
&+ \rho^3 D_{26} (X_{m,\xi\xi} Y_n X_{r,\xi} Y_{s,\eta} + X_{m,\xi} Y_{n,\eta} X_{r,\xi\xi} Y_s) \left. \right] d\xi d\eta \\
L_{ij} &= U_{T,mnrs} = \frac{a^2}{4} \int_{-1}^1 \int_{-1}^1 X_{m,\xi} Y_n X_{r,\xi} Y_s d\xi d\eta \\
m, r &= 1, 2, \dots, M, \quad n, s = 1, 2, \dots, N \\
i &= l(r-1) + s, \quad j = l(m-1) + n, \\
l &= 1, 2, \dots, M; \quad i, j = 1, 2, \dots, M \times N
\end{aligned} \tag{10}$$

167 The eigenvalue problem is then solved for λ and the critical buckling load (N_x^{cr})
168 is given by the lowest non-zero eigenvalue (λ_{cr}) of Eq. (9). The nondimensional
169 buckling coefficient is defined by,
170

$$K_x^{cr} = \frac{N_x^{cr} b^2}{\pi^2 \sqrt{D_{11} D_{22}}} \tag{11}$$

171 The RR method applied to anisotropic plates with low flexural-twist anisotropy
172 converged to an accurate buckling load results with few Legendre polynomials.
173 But, for plates with high flexural twist anisotropy, the convergence of the RR
174 method became very slow due to the difficulty associated in satisfying the nat-
175 ural boundary conditions along the edges of the plate and the highly localised
176 deformations near the boundaries. Also, the numerical ill-conditioning problem
177 associated with use of more terms to get satisfactory results limits the practical
178

179 benefits of the RR method. Therefore, new methodologies have to be developed
 180 to overcome the convergence problems of the RR method which are explained in
 181 the subsequent sections.

182 THE LAGRANGIAN MULTIPLIER METHOD

183 The methodology using Lagrangian multipliers (LM) based on Budiansky's
 184 approach (Budiansky and Hu 1946) was extended to study the effect of flexural-
 185 twist anisotropy on buckling load solutions. In the RR method, the coefficient
 186 terms of Legendre polynomials in Eq.(8) under different boundary conditions are
 187 functions of nondimensional coordinates which makes the admissible functions of
 188 Eq. (6) non-orthogonal and, therefore, less efficient. In this approach, the admis-
 189 sible functions, expanded as a series are forced to satisfy the essential boundary
 190 conditions using Lagrangian multipliers rather than term by term satisfaction of
 191 boundary conditions, as in the RR method. This approach results in both orthog-
 192 onality of admissible functions and satisfaction of essential boundary conditions.
 193 In this work, the admissible functions of Eq. (6) are expanded using Legendre
 194 polynomials directly, $X_m = P_m(\xi)$, $Y_n = P_n(\eta)$ and the functional of Eq. (3)
 195 becomes,

$$196 \quad \Pi_{LM} = U_b + \lambda U_T + \sum_{p,q} \Lambda \cdot H(A_{mn}) \quad (12)$$

197 where Λ is a Lagrangian Multiplier and $H(A_{mn})$ is a function of undetermined
 198 coefficients (A_{mn}), which are related to the boundary conditions. The terms
 199 p, q denote the number of Lagrangian Multipliers used for the constrained edges.
 200 The geometric boundary conditions along the edges are discretized independently
 201 using admissible functions and they are forced to be satisfied using Lagrangian
 202 multipliers. For example, the boundary condition ($w = 0$ at $\xi = 1$) for a simply-
 203 supported edge are

$$\begin{aligned}
& \sum_m^M \sum_n^N A_{mn} X_m(1) Y_n(\eta) = 0 \Rightarrow \\
& \sum_m^M A_{m1} X_m(1) Y_1(\eta) = 0, \quad \sum_m^M A_{m2} X_m(1) Y_2(\eta) = 0, \dots \\
& \sum_m^M A_{mp} X_m(1) Y_p(\eta) = 0, \dots \\
& \Rightarrow \sum_p^P \Lambda_p \sum_m^M A_{mp} X_m(1) = 0 \quad (p = 1, 2, \dots, P \leq N)
\end{aligned} \tag{13}$$

204 For a SSSS plate, the last term in Eq. (12) is expressed as,

$$\begin{aligned}
& \sum_{p,q} \Lambda H(A_{mn}) = \\
& \sum_{p_1}^P \Lambda_{p_1} \sum_m^M A_{mp_1} + \sum_{p_2}^P \Lambda_{p_2} \sum_m^M A_{mp_2} (-1)^{m+1} \\
& + \sum_{q_1}^Q \Lambda_{q_1} \sum_n^N A_{q_1 n} + \sum_{q_2}^Q \Lambda_{q_2} \sum_n^N A_{q_2 n} (-1)^{n+1} \\
& (P < N; Q < M)
\end{aligned} \tag{14}$$

207 where p_1, p_2, q_1, q_2 denote the number of Lagrangian Multipliers that are used
208 to constrain the deflection boundary conditions along the edges of $\xi = 1, \xi =$
209 $-1, \eta = 1, \eta = -1$, respectively.

210 Other boundary conditions are captured in a similar way. After the minimiz-
211 ing process, the following matrix expression is obtained,

$$\left\{ \left[\begin{array}{cc} \mathbf{K} & \mathbf{H} \\ \mathbf{H}^T & \mathbf{O} \end{array} \right] + \lambda \left[\begin{array}{cc} \mathbf{L} & \mathbf{O} \\ \mathbf{O} & \mathbf{O} \end{array} \right] \right\} \left\{ \begin{array}{c} \mathbf{A} \\ \mathbf{\Lambda} \end{array} \right\} = 0 \tag{15}$$

213 where matrix $[\mathbf{O}]$ is the null matrix and $[\mathbf{A}]$, $[\mathbf{K}]$, $[\mathbf{L}]$ are defined in Eq. (9)

214 and (10). $[\Lambda]$ is the set of Lagrange Multipliers. The term λ is the eigenvalue
 215 of buckling load. Dimensions of the matrices $[\mathbf{K}]$, $[\mathbf{H}]$, $[\mathbf{L}]$ are $MN \times MN$,
 216 $MN \times 2(P + Q)$, $MN \times MN$ respectively.

217 Elements in matrix \mathbf{H} are given as follows, in which the row index (i) is defined
 218 in Eq. (10) and the column index $j = l(p_1 + p_2) + (q_1 + q_2)$.

$$219 \quad H_{ij}(j \leq 2P) = \begin{cases} (-1)^{r+1} & j = 2s - 1 \\ 1 & j = 2s \\ 0 & \text{others} \end{cases} \quad (16)$$

$$220 \quad H_{ij}(j > 2P) = \begin{cases} (-1)^{s+1} & j = 2r - 1 \\ 1 & j = 2r \\ 0 & \text{others} \end{cases} \quad (17)$$

221 The number of Lagrangian multipliers along each edge (P or Q) is required to be
 222 less than the number of terms of admissible functions (M or N). By altering the
 223 values of P and Q , the upper and lower bounds of critical buckling load (N_x^{cr})
 224 are obtained. The merits of using Lagrangian multipliers are: (i) improvements
 225 in the convergence of the RR method. (ii) identification of upper and lower
 226 bounds of the critical buckling loads. Another way to address the convergence
 227 problem of buckling of composite plates with high flexural-twist anisotropy is
 228 to rely on generalised variational principles such as that explained in the next
 229 section(Washizu 1975).

230 **HELLINGER-REISSNER VARIATIONAL PRINCIPLE**

231 The slow convergence of the RR method on anisotropic plates, discussed in
 232 the RR formulation section, is mainly due to none satisfaction of natural (force)
 233 boundary conditions and the highly localised deformation in the vicinity of bound-
 234 aries. We now use the variational form, given by Hellinger and Reissner (Reissner

235 1950), to solve the buckling problem of anisotropic plates. The H-R principle, in
 236 terms of out-of-plane deflection and bending moments, is given by

$$\begin{aligned}
 \Pi_{HR} = \iint_S \left\{ \left(-M_x \frac{\partial^2 w}{\partial x^2} - M_y \frac{\partial^2 w}{\partial y^2} - M_{xy} \frac{\partial^2 w}{\partial x \partial y} \right) \right. \\
 237 \quad - \frac{1}{2} (d_{11} M_x^2 + d_{22} M_y^2 + 2d_{12} M_x M_y + 2d_{16} M_x M_{xy} \\
 \quad \left. + 2d_{26} M_y M_{xy} + d_{66} M_{xy}^2) \right\} dx dy \quad (18)
 \end{aligned}$$

238 where d_{ij} ($i, j = 1, 2, 6$) is the bending compliance (D^{-1}) defined as,

$$239 \quad \begin{bmatrix} d_{11} & d_{12} & d_{16} \\ d_{12} & d_{22} & d_{26} \\ d_{16} & d_{26} & d_{66} \end{bmatrix} = \begin{bmatrix} D_{11} & D_{12} & D_{16} \\ D_{12} & D_{22} & D_{26} \\ D_{16} & D_{26} & D_{66} \end{bmatrix}^{-1} \quad (19)$$

240 The bending moments M_x, M_y, M_{xy} are allowed to vary independently in Eq. (18)

241 and expanded in nondimensional form by the following expression,

$$\begin{aligned}
 M_x &\rightarrow M_\xi(\xi, \eta) = \sum_{m=1}^{M_1} \sum_{n=1}^{N_1} \phi_{mn}^{(a)} X_m^{(a)}(\xi) Y_n^{(a)}(\eta) \\
 242 \quad M_y &\rightarrow M_\eta(\xi, \eta) = \sum_{m=1}^{M_2} \sum_{n=1}^{N_2} \phi_{mn}^{(b)} X_m^{(b)}(\xi) Y_n^{(b)}(\eta) \\
 M_{xy} &\rightarrow M_{\xi\eta}(\xi, \eta) = \sum_{m=1}^{M_3} \sum_{n=1}^{N_3} \phi_{mn}^{(c)} X_m^{(c)}(\xi) Y_n^{(c)}(\eta)
 \end{aligned} \quad (20)$$

243 where M_1, N_1, \dots, N_3 denote the total number used for each admissible function
 244 $X_m^{(a)}, Y_n^{(a)}, \dots, Y_n^{(c)}$ of the bending moments, respectively. Substituting Eq. (6)
 245 and (20) into Eq. (18) and performing the usual minimizing procedure, a set of
 246 algebraic equations in matrix form is given as

247

$$\left\{ \left[\begin{array}{cc} \mathbf{O} & \mathbf{B} \\ \mathbf{B}^T & \mathbf{C} \end{array} \right] + \lambda \left[\begin{array}{cc} \mathbf{L} & \mathbf{O} \\ \mathbf{O} & \mathbf{O} \end{array} \right] \right\} \left\{ \begin{array}{c} \mathbf{A} \\ \Phi \end{array} \right\} = 0 \quad (21)$$

248 where $[\mathbf{L}]$ is defined in Eq. (10). Matrix $[\mathbf{A}]$ and $[\Phi] = [\phi_{11}^{(a)}, \phi_{12}^{(a)}, \dots, \phi_{M_1 N_1}^{(a)},$
 249 $\phi_{11}^{(b)}, \phi_{12}^{(b)}, \dots, \phi_{M_2 N_2}^{(b)}, \phi_{11}^{(c)}, \phi_{12}^{(c)}, \dots, \phi_{M_3 N_3}^{(c)}]^T$ are the undetermined coefficients of
 250 deflection and moments, respectively. Again, λ is the eigenvalue of buckling
 251 load as defined in Eq. (3) and (15). Dimensions of the matrices $[\mathbf{B}]$ and $[\mathbf{C}]$ are
 252 $MN \times (M_1 N_1 + M_2 N_2 + M_3 N_3)$, $(M_1 N_1 + M_2 N_2 + M_3 N_3) \times (M_1 N_1 + M_2 N_2 + M_3 N_3)$
 253 respectively.

254 Matrix $[B]$ contains three submatrices, $[B] = [B_{11} \ B_{12} \ B_{13}]$ and are given
 255 by,

$$\begin{aligned} B_{11,mnrs} &= \int_{-1}^1 \int_{-1}^1 X_m \xi \xi Y_n X_r^{(a)} Y_s^{(a)} d\xi d\eta \\ B_{12,mnrs} &= \int_{-1}^1 \int_{-1}^1 X_m Y_n \eta \eta X_r^{(b)} Y_s^{(b)} d\xi d\eta \\ B_{13,mnrs} &= \int_{-1}^1 \int_{-1}^1 X_m \xi Y_n \eta X_r^{(c)} Y_s^{(c)} d\xi d\eta \end{aligned} \quad (22)$$

257 Matrix $[C]$ contains nine submatrices which are defined using,

$$[\mathbf{C}] = \begin{bmatrix} C_{11} & C_{12} & C_{13} \\ C_{12}^T & C_{22} & C_{23} \\ C_{13}^T & C_{23}^T & C_{33} \end{bmatrix} \quad (23)$$

258

259

$$\begin{aligned}
C_{11,mnrs} &= \int_{-1}^1 \int_{-1}^1 X_m^{(a)} Y_n^{(a)} X_r^{(a)} Y_s^{(a)} d\xi d\eta \\
C_{12,mnrs} &= \int_{-1}^1 \int_{-1}^1 X_m^{(a)} Y_n^{(a)} X_r^{(b)} Y_s^{(b)} d\xi d\eta \\
C_{13,mnrs} &= \int_{-1}^1 \int_{-1}^1 X_m^{(a)} Y_n^{(a)} X_r^{(c)} Y_s^{(c)} d\xi d\eta \\
C_{22,mnrs} &= \int_{-1}^1 \int_{-1}^1 X_m^{(b)} Y_n^{(b)} X_r^{(b)} Y_s^{(b)} d\xi d\eta \\
C_{23,mnrs} &= \int_{-1}^1 \int_{-1}^1 X_m^{(b)} Y_n^{(b)} X_r^{(c)} Y_s^{(c)} d\xi d\eta \\
C_{33,mnrs} &= \int_{-1}^1 \int_{-1}^1 X_m^{(c)} Y_n^{(c)} X_r^{(c)} Y_s^{(c)} d\xi d\eta
\end{aligned} \tag{24}$$

260 Finally, separate expressions for the deflection function (w) and bending moments
261 (M_x, M_y, M_{xy}) are applied to Eqs. (18)-(24), such that both the deflection and
262 moment boundary conditions are satisfied. For example, using Legendre polyno-
263 mials, the moment functions for the SS or free edges are assumed to be,

$$\begin{aligned}
M_\xi(\xi, \eta) &= \sum_{m=1} \sum_{n=1} \phi_{mn}^{(a)} (1 - \xi^2) P_m(\xi) P_n(\eta) \\
M_\eta(\xi, \eta) &= \sum_{m=1} \sum_{n=1} \phi_{mn}^{(b)} P_m(\xi) (1 - \eta^2) P_n(\eta) \\
M_{\xi\eta}(\xi, \eta) &= \sum_{m=1} \sum_{n=1} \phi_{mn}^{(c)} P_m(\xi) P_n(\eta)
\end{aligned} \tag{25}$$

265 The advantage of this approach is that both essential and natural boundary
266 conditions can be both modelled and satisfied independently and this helps in
267 improving the convergence of buckling problems.

268 DIFFERENTIAL QUADRATURE METHOD

269 The differential quadrature method (DQM) was introduced by Bellman and
270 Casti (Bellman 1971) to solve initial and boundary value problems. In DQM,

271 the derivative of a function, with respect to a space variable at a given discrete
 272 grid point, is approximated as a weighted linear sum of the function values at
 273 all of the grid points in the entire domain of that variable. The n^{th} order partial
 274 derivative of a function $f(x)$ at the i^{th} discrete point is approximated by

$$275 \quad \frac{\partial^n f(x_i)}{\partial x^n} = A_{ij}^{(n)} f(x_j) \quad i = 1, 2, \dots, N \quad (26)$$

276 where x_i = set of discrete points in the x direction; and $A_{ij}^{(n)}$ is the weighting
 277 coefficients of the n^{th} derivative and repeated index j indicates summation from
 278 1 to N . The choice of the grid distribution for computation of weighting coefficient
 279 matrices and methods to model multiple boundary conditions are discussed by
 280 Shu (Shu 2000). DQM is fast and computationally less expensive to achieve
 281 results with similar levels of accuracy as variational methods. In this work, the
 282 non uniform grid distribution given by the Chebyshev-Gauss-Labotto points are
 283 used for the computation of weighting matrices and is given by

$$284 \quad X_i = \frac{1}{2} \left[1 - \cos\left(\frac{i-1}{N-1}\pi\right) \right] \quad i = 1, 2, \dots, n \quad (27)$$

285 where n is the number of grid points. The DQM representation of Eq. (1) is
 286 given by

$$287 \quad \begin{aligned} & D_{11} \sum_{k=1}^{n_x} A_{ik}^{(4)} w_{kj} + 2(D_{12} + 2D_{66}) \sum_{k=1}^{n_x} \sum_{m=1}^{n_y} A_{ik}^{(2)} B_{jm}^{(2)} w_{km} + D_{22} \sum_{m=1}^{n_y} B_{jm}^{(4)} w_{im} \\ & + 4D_{16} \sum_{k=1}^{n_x} \sum_{m=1}^{n_y} A_{ik}^{(3)} B_{jm}^{(1)} w_{km} + 4D_{26} \sum_{k=1}^{n_x} \sum_{m=1}^{n_y} A_{ik}^{(1)} B_{jm}^{(3)} w_{km} = \bar{N}_x \sum_{k=1}^{n_x} A_{ik}^{(2)} w_{kj} \end{aligned} \quad (28)$$

$$i = 1, \dots, n_x; \quad j = 1, \dots, n_y$$

288 where $A_{ik}^{(n)}, B_{jm}^{(n)}$ represent the contributions of the n^{th} order partial derivatives

289 with respect to x and y directions, respectively. The boundary conditions can
290 be written in DQM form analogously. Eq. (28) shows that DQM reduces the
291 governing differential equation into a set of algebraic equations and provides
292 an attractive procedure for solving the buckling problem. In this work, DQM
293 was applied to study the buckling of laminated plates with strong flexural-twist
294 anisotropy and the accuracy of the results was investigated.

295 **NUMERICAL RESULTS AND DISCUSSION**

296 **Highly flexurally anisotropic plate**

297 In this work, symmetrical laminates made from P100/AS3501 prepreg ma-
298 terial, which has potentially high levels of anisotropy in laminated structures,
299 (Weaver 2006) was studied under different boundary conditions. The material
300 properties of P100/AS3501 are $E_{11}=369\text{GPa}$, $E_{22}=5.03\text{GPa}$, $G_{12}=5.24\text{GPa}$ and
301 $\nu_{12}=0.31$. The proposed approaches were applied to obtain the buckling solu-
302 tions of flexurally anisotropic plates with unidirectional layups ($[+\theta]_n$). Bounds
303 of the nondimensional parameters associated with flexural-twist anisotropy for
304 the P100/AS3501 material are: $0 < |\gamma, \delta| < 0.92$ for $[+\theta]_n$ layups (Weaver and
305 Nemeth 2007). Finite Element (FE) analysis was carried out using ABAQUS for
306 validation of the proposed approaches. An 8-noded shell element with reduced
307 integration (S8R5) was chosen to discretise the plate for buckling analysis and
308 mesh density is chosen to be 100×5 to get accurate results. Results were also
309 validated with respect those previously obtained (Weaver 2006; Herencia et al.
310 2010).

311 **SSSS long plate**

312 The buckling analysis of anisotropic long plates ($a/b = 5$) with SSSS bound-
313 ary conditions was carried out using RR and DQ methods. The buckling loads
314 converge to a constant value (within 5%) for aspect ratios of plates of $a/b >$

315 $3\sqrt[4]{D_{11}/D_{22}}$ (Weaver 2006). Weaver (Weaver 2006) derived two CF expres-
316 sions for obtaining approximate solutions to the buckling coefficients of the SSSS
317 anisotropic long plate and also developed an iterative method to compute what
318 was shown to be, within a small margin, an exact value. Later, Herencia *et al*
319 (Herencia et al. 2010) derived another CF expression for this case and achieved
320 better approximate closed form solutions. The buckling results obtained by the
321 RR method with Legendre polynomials, DQM, and Herencia *et al's* CF formu-
322 lation (Eq. 29) for different fibre orientations closely matches the FE results as
323 shown in Fig. 2. The mode shape of the $[+45]_n$ SSSS long plate computed by the
324 RR method is validated by the appropriate FE result shown in Fig. 3. Therefore,
325 the effect of flexural-twist anisotropy is well captured for long anisotropic plates
326 using Herencia *et al* (Herencia et al. 2010) CF expressions with SSSS boundary
327 conditions, given by

$$328 \quad K_x^{cr} = 2\sqrt{1 - 4\delta\gamma - 3\delta^4 + 2\delta^2\beta} + 2(\beta - 3\delta^2) \quad (29)$$

329 **SSSS square plate**

330 Numerical results of nondimensional buckling coefficients of an SSSS anisotropic
331 square plate for angle-ply laminates computed by FE, DQM, RR and LM meth-
332 ods as well as the H-R principle are listed in Table 1. It is noted that to the
333 authors' best knowledge no CF solutions exist. Error percentages in buckling
334 coefficients for each method when compared with FE results are shown in Table
335 1. In DQM, the number of grid points was chosen to be $n_x, n_y = 31$ for the anal-
336 ysis. The unidirectional laminates with a ply angle of 45° exhibit high values of
337 both D_{16} and D_{26} flexural-twist anisotropy and causes very slow convergence of
338 the RR method and DQM. DQM overestimates the buckling coefficient by 11.3%
339 for the ply angles $40^\circ \sim 45^\circ$ when compared with FE results. The RR method

340 exhibits an approximately 7% error for the ply angles $40^\circ \sim 45^\circ$, even when
 341 a relatively large number (23-by-23 terms) of Legendre polynomials were used.
 342 The inability of the DQM and RR method to model the effect of flexural-twist
 343 anisotropy and the constraints due to boundary conditions are the main reasons
 344 for their failure to capture accurate results. As seen from the Table 1, both the
 345 approaches based on the LM method and the H-R principle were able to capture
 346 the above mentioned constraints and achieved buckling coefficient results with
 347 error less than 2.5%. The LM results shown in Table 1 were computed using
 348 MN=13 terms for deflection and used 11 Lagrangian multipliers to constrain the
 349 geometry boundary conditions along each edge. Fig. 4 demonstrates good con-
 350 vergence of buckling coefficients for the $[+45]_n$ SSSS square plate using the H-R
 351 variational principle with only a few polynomial terms in the admissible functions,
 352 but does not provide bounded solutions. Fig. 5 shows that the buckling mode
 353 shape of the $[+45]_n$ SSSS square plate closely matches FE when only a relatively
 354 small number of polynomial terms is used in the series. In this approach, MN
 355 (shorthand for M and N) represents the number of terms to represent deflection
 356 and moments functions requires more terms than deflection functions for obtain-
 357 ing solutions. The H-R results presented in Table 1 were computed using MN=7
 358 terms for deflection and MN+2 terms for moment functions and the results did
 359 not exhibit bounded solution because of the variation of convergence behaviour
 360 with ply layups. Therefore, by choosing an appropriate number of polynomials
 361 in both approaches, results with good accuracy can be achieved.

362 **SSSF long plate**

363 Numerical results of a long anisotropic plate ($a/b = 20$) with SSSF bound-
 364 ary conditions for all unidirectional layups are presented in this section. The
 365 FE results (Fig. 6) show that two possible buckling mode shapes exists and

366 so confirms preliminary results (Weaver and Herencia 2007). The first mode
 367 shape is asymmetrical, largely skewed to one side of the plate and the alternative
 368 mode shape is nearly symmetrical in nature. For the laminates with ply angle
 369 less than 45° , the D_{16} bending-twist anisotropy is high and the plate exhibits
 370 a shear instability near the boundary resulting in twisting of the free edge to
 371 one side of the plate. But, for laminates with layup greater than 45° , the D_{16}
 372 bending-twist anisotropy is relatively low and the plate exhibits almost symmet-
 373 rical bending behavior of the free edge similar to orthotropic plates. Weaver and
 374 Herencia (Weaver and Herencia 2007) proposed one-term expressions to approx-
 375 imately represent each mode shape in Fig. 6. By assuming the mode shape with
 376 one side skewed to be $w = w_0 e^{-qx/a} \sin(m\pi x/a)y$ and the second mode shape as
 377 $w = w_0 \sin(m\pi x/a - ky)y$, the following CF solutions of buckling coefficient were
 378 derived and are given by,

$$K_x^{cr} = 12\epsilon - \frac{36}{5}\gamma^2 \quad (\text{CF1}) \quad (30)$$

$$K_x^{cr} = 12\epsilon - 12\delta^2 \quad (\text{CF2})$$

380 where $\epsilon = D_{66}/\sqrt{D_{11}D_{22}}$. Further insight into these two mode shapes can be
 381 obtained as follows. By considering the zero moment boundary condition and
 382 $\kappa_y = 0$ along the short edge where the mode shape is skewed, the following
 383 relations along this boundary are obtained, as

$$\begin{aligned}
 M_x &= D_{11}\kappa_x + D_{12}\kappa_y + D_{16}\kappa_{xy} = 0 \Rightarrow \\
 \kappa_x &= -\frac{D_{16}}{D_{11}}\kappa_{xy} \Rightarrow \\
 M_{xy} &= D_{16}\kappa_x + D_{26}\kappa_y + D_{66}\kappa_{xy} = (D_{66} - \frac{D_{16}^2}{D_{11}})\kappa_{xy}
 \end{aligned} \quad (31)$$

385 where $\kappa_x, \kappa_y, \kappa_{xy}$ are bending curvatures of plate. Such analysis shows that the
 386 effective twisting stiffness, D_{66} is reduced by the presence of D_{16} . Examining the
 387 form of CF1 shows the same functional dependence on D_{66} , D_{11} and D_{16} but the
 388 effective twisting stiffness defined in Eq. (31) is less than that given by CF1. A
 389 similar formula to CF1 is obtained directly from the orthotropic buckling formula
 390 (Weaver and Herencia 2007) but substituting the reduced torsional stiffness from
 391 Eq. (31) for D_{66} . Examining the skewed mode shape in Fig. 6 shows the shear
 392 instability is in the proximity of the short edge where both M_x and κ_y are close
 393 to zero. However, the maximum buckling amplitude is a short distance from
 394 the edge where these conditions are no longer exactly satisfied and the effective
 395 torsional stiffness would be expected to be larger than the lower bound value
 396 given by Eq. (31). As such, it is expected that the true buckling load to lie
 397 between CF1 and the lower bound value using Eq. (31) for the torsional stiffness.
 398 Thus, CF1 in Eq. 30 is modified to

$$399 \quad K_x^{cr} = [12\epsilon - 12\gamma^2] \text{ (CF-lowerbound)} \quad (32)$$

400 which usurps, and improves upon, the empirical CF formula given in Weaver
 401 and Herencia 2007. Furthermore, an analogous argument along the long, simply
 402 supported edge (M_y and $\kappa_x = 0$) provides a torsional stiffness reduced by the
 403 presence of D_{26} . In fact, if this reduced torsional stiffness is substituted for D_{66}
 404 then one obtains CF2 directly.

405 The numerical results computed using the RR method, Weaver's CF expres-
 406 sions (Weaver and Herencia 2007), DQM and FE analysis are shown in Fig. 7.
 407 For ply angles larger than 45° , Weaver's CF solutions, RR and DQM results
 408 matches well with the FE results. However, when ply angles are in the range of

409 $10^\circ \sim 40^\circ$, the results of all the methods show large inaccuracy compared with
 410 FE. For the case of $[+30]_n$, the RR method used 23 by 23 terms of Legendre
 411 polynomials in the admissible functions and the error was found to be in excess
 412 of 25% when compared with FE results. Using more Legendre polynomial terms
 413 is beyond the precision of our current computer capacity and leads to numerical
 414 ill-conditioning problems.

415 For laminates with ply angles larger than 40° , the buckling mode shape eval-
 416 uated by all of the methods were found to be similar to the second mode shape
 417 shown in Fig. 6 and the buckling coefficients matched the FE results. For lam-
 418 inates with ply angle less than 40° , the first buckling mode shape as shown in
 419 Fig. 6 was found to be skewed to one side of the plate and the RR method
 420 was not able to capture the mode shape accurately resulting in non-physical high
 421 buckling coefficient values, as shown in Fig.7. In addition, there were difficulties
 422 in representing the mode shape analytically in this angle range and the critical
 423 buckling loads computed using analytical methods become very sensitive to the
 424 assumption of mode shape functions. Buckling analysis carried out by DQM
 425 could only capture the second symmetric mode shape and resulted in over es-
 426 timation of buckling load. The above results indicate that a robust numerical
 427 methodology has to developed to solve the buckling load solutions of laminated
 428 plates with strong flexural-twist anisotropy.

429 To this end, the extreme case of $[+30]_n$ SSSF long plate ($a/b = 20$) was
 430 analysed in detail using the Lagrangian multiplier approach. The number of
 431 Lagrangian multipliers along the edges in Eq. (12) were chosen to be 2 – 6 less
 432 than the number of terms used in admissible functions ($P=Q=PQ, M=N=MN,$
 433 $PQ=MN-2 \dots - 6$). When all the boundary conditions in Eq. (14) were fully
 434 satisfied by using Lagrangian multipliers, the plate becomes stiffer and gives an
 435 upper bound solution. When the number of Lagrangian multipliers is reduced,

436 constraints on the plate, along the edges, are relaxed and it results in a lower
 437 estimation of buckling load. Fig. 8 illustrate the convergence trend of buckling
 438 coefficients (K_x^{cr}) by varying the number of Lagrangian multipliers. The upper
 439 and lower bounds of K_x^{cr} of $[+30]_n$ SSSF long plate are found in Fig. 8, for
 440 this case an exact solution is not possible and the RR method suffers very slow
 441 convergence. It can be seen that the FE result falls within the obtained bounds
 442 computed by this approach and can be used to confirm accurate buckling load
 443 results.

444 In the H-R variational principle approach, the accuracy and convergence of
 445 the buckling load results are studied for the $[+30]_n$ SSSF long plate ($a/b = 20$)
 446 by varying the number of terms of Legendre polynomials to represent deflection
 447 and moments. Fig. 9 demonstrates good convergence of the buckling coefficients
 448 towards FE results using this approach. The mode shape as shown in Fig. 10
 449 was computed using few polynomial terms (5 or 10) for the deflection function
 450 and closely matches the FE solution. Hence, the above approach gives valuable
 451 insight in to the number of terms in deflection and moment functions to get
 452 better results. By using more terms to represent the moment functions than
 453 the deflection function makes the plate stiffer and always results in upper bound
 454 solution to the FE result.

455 Figs. 8 and 9 shows that the accuracy of buckling solutions when compared
 456 with FE results is affected by the chosen number of Lagrangian multipliers and
 457 the number of terms used in moment functions. Hence, appropriately choosing
 458 the number of these terms is important for the robustness of both proposed ap-
 459 proaches. The optimal number can be selected based on that which gives good
 460 convergence (i.e. upper or lower bound). The proposed approaches works well
 461 for plates with low flexural anisotropy and exhibits convergence similar to the
 462 RR approach. For the case of laminated plates with extremely high flexural

463 anisotropy studied in this paper, the proposed approaches can be used as bench-
 464 marks to choose the number of Legendre polynomials for representing deflection
 465 functions, moment functions and Lagrangian multipliers. The chosen number of
 466 terms varies with different plate boundary conditions. For the buckling problem
 467 of SSSF long plate: (i) 21 terms of Legendre polynomials for the deflection func-
 468 tion (MN) and 17 Lagrangian multipliers (PQ) along each edge were chosen in
 469 the LM method; (ii) in the H-R principle, 10 terms for deflection function and 13
 470 terms for each moment function ($M_i N_i = 13$) were used. These selections were
 471 based on the results presented in Figs. 8 and 9 for the $[+30]_n$ SSSF long plate.
 472 Both the LM method and the H-R principle were then applied to all the angle
 473 orientations of the SSSF long plate ($[+\theta]_s$) and the results are shown in Fig. 11.
 474 The buckling load solutions obtained using these two approaches closely match
 475 the FE solutions for all the angle-ply orientations. The results obtained using the
 476 H-R variational principle were closer to the FE result than the LM approach.

477 CONCLUSION

478 The buckling problems of anisotropic plates with strong flexural-twist coupling
 479 under different boundary conditions have been investigated. The drawbacks of
 480 both DQM and the RR method to accurately model constraints due to high
 481 flexural-twist anisotropy for some specific cases ($[+45]_n$ SSSS square plate and
 482 $[+30]_n$ SSSF long plate) were discussed. In these cases, the distorted buckling
 483 mode shapes were difficult to represent analytically (due to localised deforma-
 484 tions) and the CF solutions were unable to predict correct buckling load results.
 485 In order to model these problems accurately, two numerical methodologies based
 486 on the Lagrangian multiplier concept and Hellinger-Reissner variational principle
 487 were proposed. In the LM approach, the orthogonality of the admissible functions
 488 and satisfaction of essential boundary conditions along the edges were ensured

489 by selecting appropriate Lagrangian multiplier terms. The most important ad-
490 vantage of this approach was its ability to provide the upper and lower bounds
491 of buckling coefficient. This approach also ensured fast convergence of buckling
492 load solution by using few polynomials when compared to the RR method.

493 In the approach based on the Hellinger-Reissner variational principle, both the
494 essential and natural boundary conditions were captured effectively. The most
495 distinct advantage of using this approach is that it can obtain accurate results
496 with very limited number of terms in the admissible functions when compared
497 to other approaches. On the other hand, the variational principle also has some
498 issues for the buckling analysis of composite plates. For example, it can generate
499 different levels of convergence when choosing different numbers of terms in the ad-
500 missible functions, which makes them difficult to identify converged results. The
501 efficiency will be significantly decreased with an increase of number of terms, as it
502 requires a significantly larger matrix (to invert) than the RR method. However,
503 the mixed variational approach provides insight in to the study of flexural-twist
504 anisotropy on buckling solutions.

505 Finally, a closed form formula has been offered as a lower bound estimate of
506 buckling load of a long, simply supported, flexurally anisotropic plate, with one
507 long edge free.

508 REFERENCES

- 509 Ashton, J. (1969). "Analysis of anisotropic plates 2." *Journal of Composite Ma-*
510 *terials*, 3(3), 470–479.
- 511 Ashton, J. and Waddoups, M. (1969). "Analysis of anisotropic plates." *Journal*
512 *of Composite Materials*, 3(1), 148–165.
- 513 Balabuch, L. (1937). "The stability of plywood plates." *Aeronautical Engineering*,
514 *USSR*, 11.

- 515 Bellman, R.E. & Casti, J. (1971). “Differential quadrature and long-term inte-
516 gration.” *J Math Anal Appl*, Vol. 34, 235?.
- 517 Bhat, R. (1985). “Natural frequencies of rectangular plates using characteristic
518 orthogonal polynomials in Rayleigh-Ritz method..” *Journal of Sound and Vi-*
519 *bration*, 102(4), 493 – 499.
- 520 Budiansky, B. and Hu, P. C. (1946). “The lagrangian multiplier method of finding
521 upper and lower limits to critical stresses of clamped plates.” *NACA*,, Report
522 No. 848.
- 523 Chamis, C. C. (1969). “Buckling of anisotropic composite plates.” *J. Struct. Div.*,
524 95(ST10), 2119?139.
- 525 Chien, W.-Z. (1984). “Generalized variational principles in elasticity.” *Engineer-*
526 *ing Mechanics in Civil Engineering*, 29, 93–153.
- 527 Chow, S., Liew, K., and Lam, K. (1992). “Transverse vibration of symmetrically
528 laminated rectangular composite plates.” *Composite Structures*, 20(4), 213–
529 226.
- 530 Darvizeh, M., Darvizeh, A., Ansari, R., and Sharma, C. B. (2004). “Buck-
531 ling analysis of generally laminated composite plates (generalized differential
532 quadrature rules versus RayleighRitz method).” *Composites and structures*,
533 Vol. 63, 69–74.
- 534 Green, A. and Hearmon, R. (1945). “The buckling of flat rectangular plywood
535 plates.” *Philosophical Magazine*, 7, 659–688.
- 536 Grenestedt, J. L. (1989). “Study on the effect of bending-twisting coupling on
537 buckling strength.” *Composite Structures*, 12(4), 271 – 290.
- 538 Herencia, J. E., Weaver, P. M., and Friswell, M. I. (2010). “Closed-form solutions
539 for buckling of long anisotropic plates with various boundary conditions under
540 axial compression.” *Journal of Engineering Mechanics*, 136(9), 1105–1114.
- 541 Liew, K. and Wang, C. (1995). “Elastic buckling of regular polygonal plates.”

542 *Thin-Walled Structures*, 21(2), 163–173.

543 Nemeth, M. P. (1986). “Importance of anisotropy on buckling of compression-
544 loaded symmetric composite plates.” *AIAA journal*, 24(11), 1831–1835.

545 Pandey, M. D. and Sherbourne, A. N. (1991). “Buckling of anisotropic composite
546 plates under stress gradient.” *Journal of Engineering Mechanics*, 117(2), 260 –
547 275.

548 Plass, H. J., Gaines, J. H., and Newsom, C. D. (1962). “Application of reissner’s
549 variational principle to cantilever plate deflection and vibration problems.”
550 *Journal of Applied Mechanics*, 29, 127–135.

551 Reissner, E. (1950). “On a variational theorem in elasticity.” *Journal of Mathe-*
552 *matics and Physics*, 29(2), 90–95.

553 Sherbourne, A. N. and Pandey, M. D. (1991). “Differential quadrature method in
554 the buckling analysis of beams and composite plates.” *Computers and Struc-*
555 *tures*, 40, 903–13.

556 Shu, C. (2000). *Differential quadrature and its application in engineering*. London:
557 Springer-Verlag.

558 Smith, S. T., Bradford, M. A., and Oehlers, D. J. (1999). “Numerical convergence
559 of simple and orthogonal polynomials for the unilateral plate buckling problem
560 using the RayleighRitz method.” *International Journal for Numerical Methods*
561 *in Engineering*, 44(11), 1685–1707.

562 Tang, W.-Y. and Sridharan, S. (1990). “Buckling analysis of anisotropic plates us-
563 ing perturbation technique.” *Journal of Engineering Mechanics*, 116(10), 2223
564 – 2236.

565 Thielemann, W. (1950). “Contribution to the problem of buckling of orthotropic
566 plates, with special reference to plywood.” *NACA Technical Memorandum*
567 *1263*.

568 Washizu, K. (1975). *Variational Methods in Elasticity and Plasticity*, second edi-

- 569 *tion*. Pergamon Press, London.
- 570 Weaver, P. M. (2006). “Approximate analysis for buckling of compression loaded
571 long rectangular plates with flexural/twist anisotropy.” *Proceedings of the Royal
572 Society A: Mathematical, Physical and Engineering Science*, 462(2065), 59–73.
- 573 Weaver, P. M. and Herencia, J. E. (2007). “Buckling of a flexurally anisotropic
574 plate with one edge free.” *AIAA/ASME/ASCE/AHS/ASC Structures, Struc-
575 tural Dynamics and Materials Conference*, 8, 8534 – 8542.
- 576 Weaver, P. M. and Nemeth, M. P. (2007). “Bounds on flexural properties and
577 buckling response for symmetrically laminated composite plates.” *Journal of
578 Engineering Mechanics*, 133(11), 1178 – 1191.
- 579 Whitney, J. (1972). “Free vibration of anisotropic rectangular plates.” *Journal of
580 the Acoustical Society of America*, 52(1 Part 2), 448 – 449.

TABLE 1. Buckling Coefficient K_x^{cr} of $[+\theta]_n$ SSSS square plate

θ	FE	DQM	RR (MN=23)	LM (MN=13) ^{†1}	H-R (MN=7) ^{‡2}
0	9.240	9.240 (0.00)	9.240 (0.00)	9.240 (0.00)	9.240 (0.00)
10	8.311	8.401 (1.08)	8.407 (1.15)	8.393 (0.98)	8.404 (1.11)
20	5.332	5.379 (0.87)	5.413 (1.51)	5.364 (0.59)	5.385 (0.99)
30	2.923	3.063 (4.82)	3.026 (3.52)	2.906 (0.59)	2.919 (0.12)
40	1.997	2.223 (11.3)	2.144 (7.36)	1.948 (2.44)	1.959 (1.91)
45	1.839	2.043 (11.1)	1.968 (7.03)	1.795 (2.40)	1.804 (1.87)
50	1.807	1.880 (4.03)	1.856 (2.71)	1.771 (1.96)	1.780 (1.49)
60	1.819	1.884 (3.58)	1.881 (3.41)	1.812 (0.40)	1.830 (0.60)
70	2.303	2.286 (0.76)	2.339 (1.56)	2.311 (0.33)	2.337 (1.45)
80	2.638	2.661 (0.88)	2.664 (1.02)	2.655 (0.68)	2.666 (1.06)
90	2.545	2.561 (0.61)	2.561 (0.61)	2.561 (0.61)	2.561 (0.62)

¹ † 11 Lagrangian multipliers were used for boundary conditions along each edge.

² ‡ 9 terms were used for each moment function.

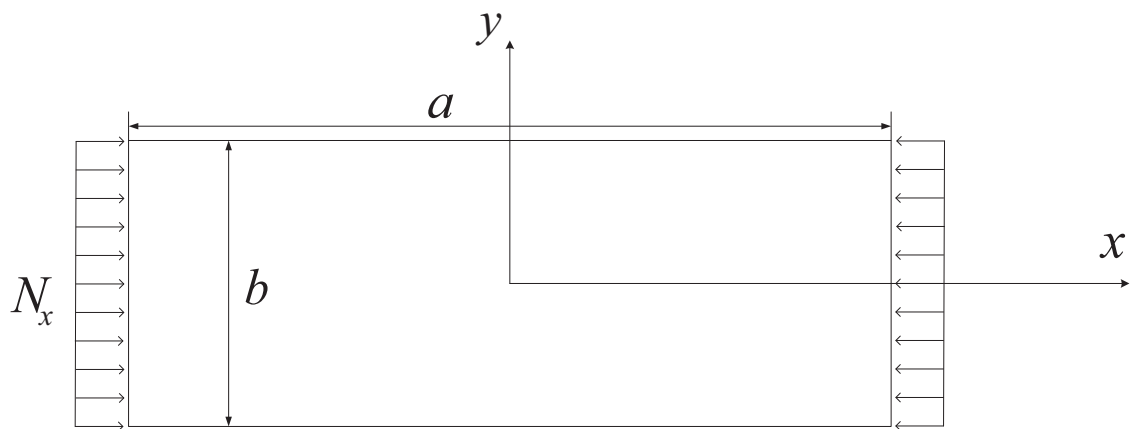


FIG. 1. Load and geometry of anisotropic plates

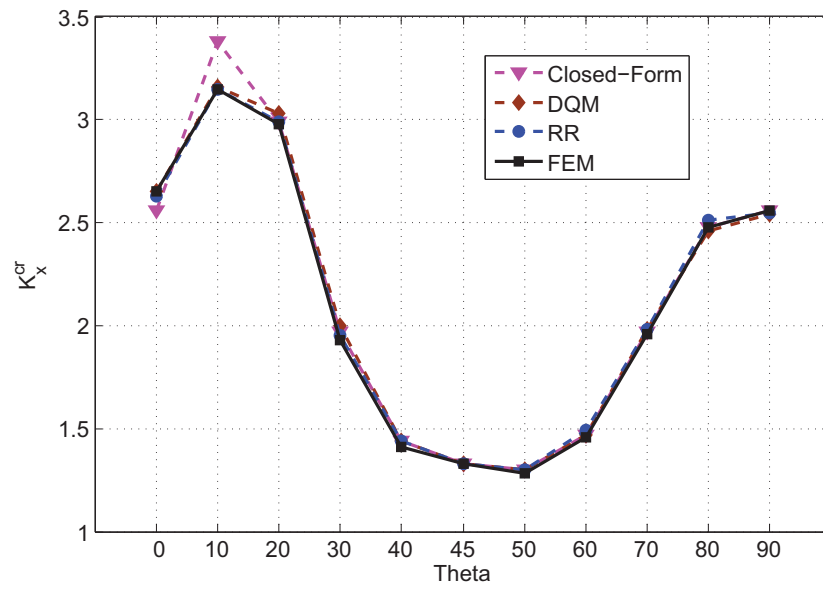


FIG. 2. Buckling coefficients vs. ply angles for $[+\theta]_n$ SSSS long plate ($a/b = 5$).

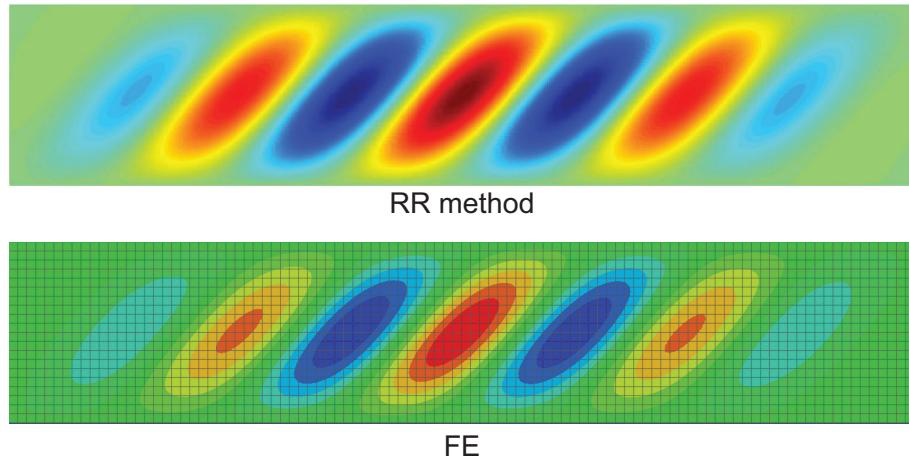


FIG. 3. Buckling mode shapes of $[+45]_n$ SSSS long plate ($a/b = 5$) obtained by RR method and FE.

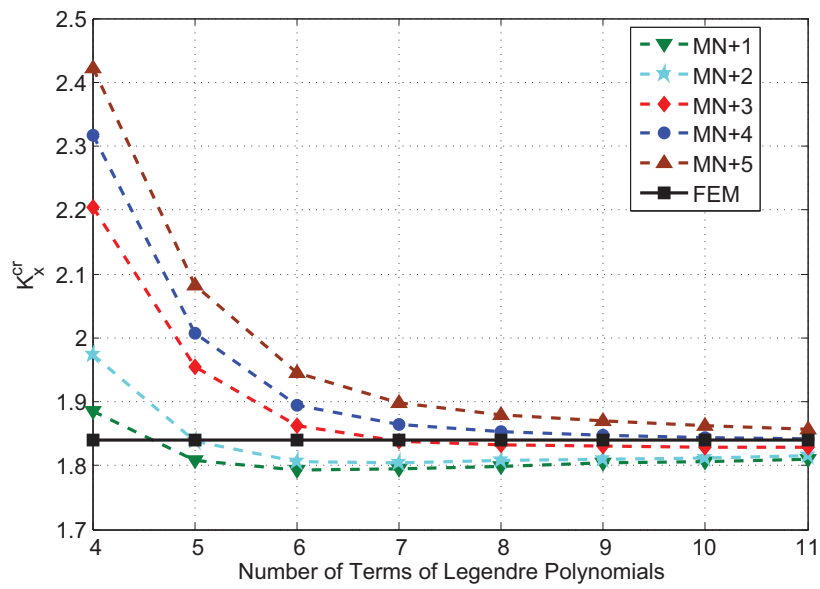
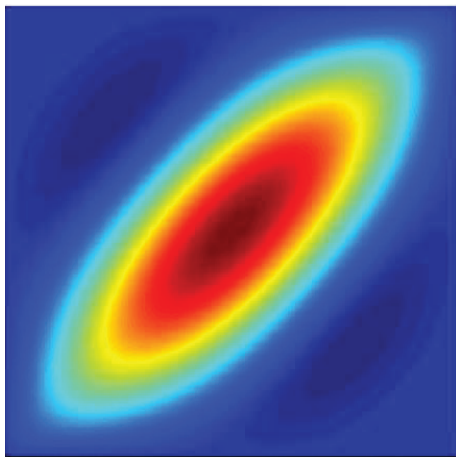
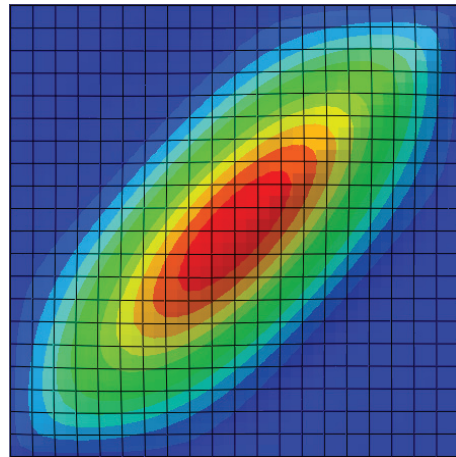


FIG. 4. The convergence trend of non-dimensional buckling coefficient (K_x^{cr}) of $[+45]_n$ SSSS square plate varying with the number of terms (M, N) in admissible functions using the H-R principle. Different curves in this plot represent different number of terms used in the moment functions where MN represents the number of terms in the deflection function.

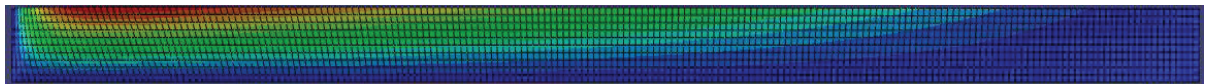


H-R principle

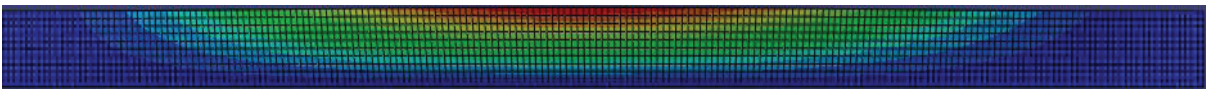


FE

FIG. 5. Buckling mode shapes of $[+45]_n$ SSSS square plate obtained by using H-R principle and FE.



Buckling Mode Shape - I (Asymmetric)



Buckling Mode Shape - II (Symmetric)

FIG. 6. Buckling mode shapes of $[+\theta]_n$ SSSF long plate (FE).

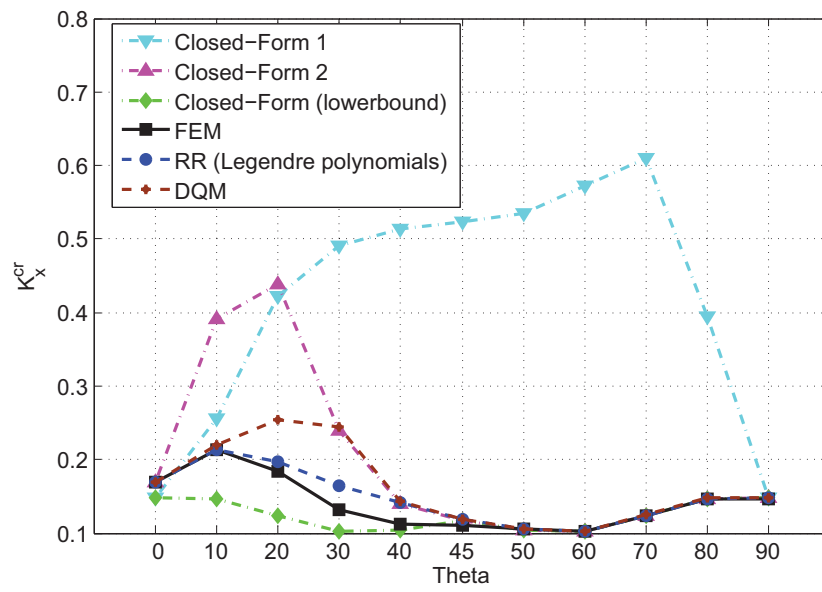


FIG. 7. Buckling coefficients vs. ply angles for $[+\theta]_n$ SSSF long plate.

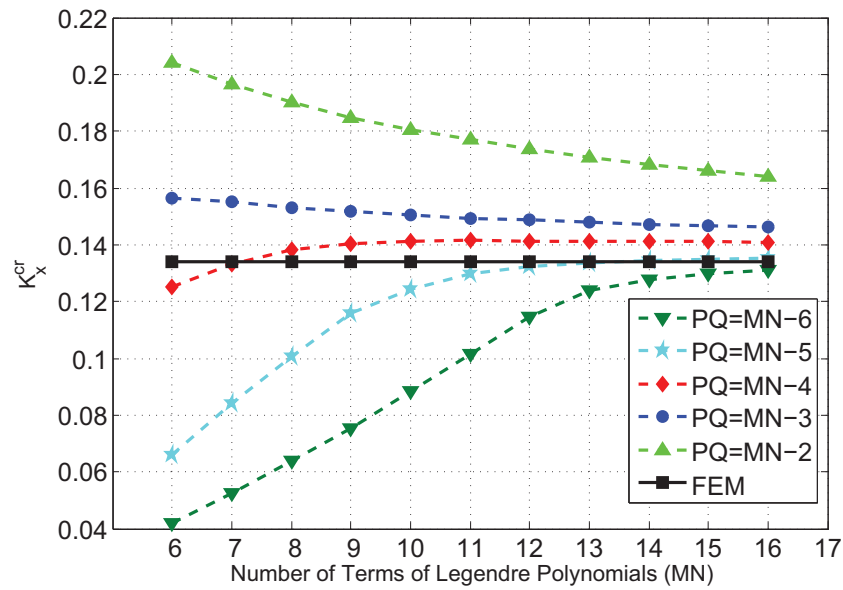


FIG. 8. The convergence trend of the non-dimensional buckling coefficient (K_x^{cr}) of $[+30]_n$ SSSF long plate ($a/b = 20$) varying with the number of terms (M, N) in admissible functions using the LM method. Different curves in this plot represent different number of Lagrangian multipliers.

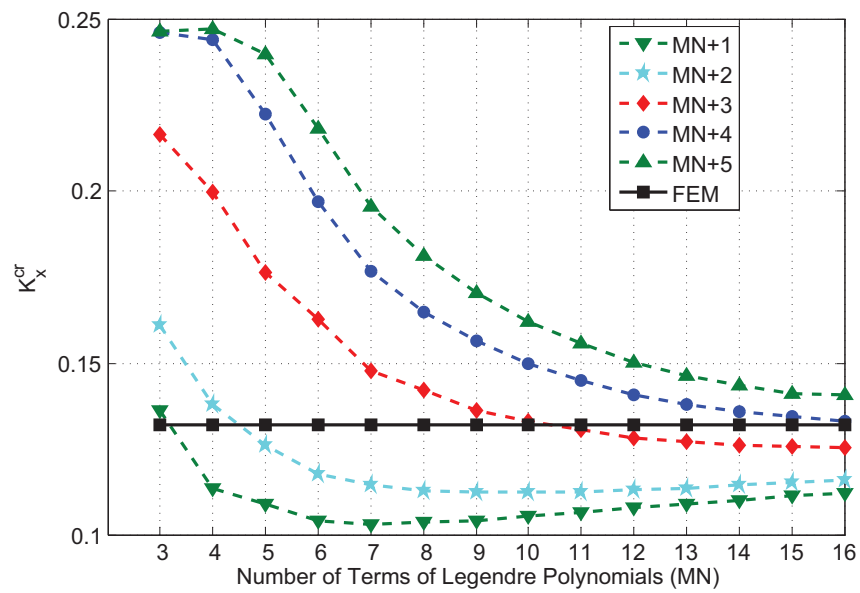


FIG. 9. The convergence trend of non-dimensional buckling coefficient (K_x^{cr}) of $[+30]_n$ SSSF long plate ($a/b = 20$) varying with the number of terms (M, N) in admissible functions using the H-R principle. Different curves in this plot represent different number of terms used in the moment functions where MN represents the number of terms in the deflection function.

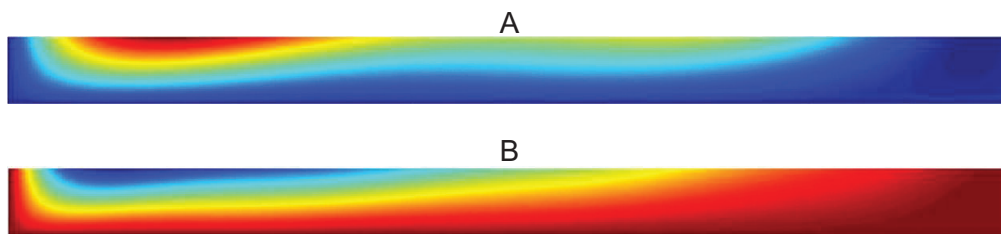


FIG. 10. The buckling mode shapes obtained using the H-R principle with different number of terms of Legendre polynomials of the admissible functions. (A) 5 terms for each deflection function and 8 terms for each moment function. (B) 10 terms for the deflection and 14 terms for each moment function.

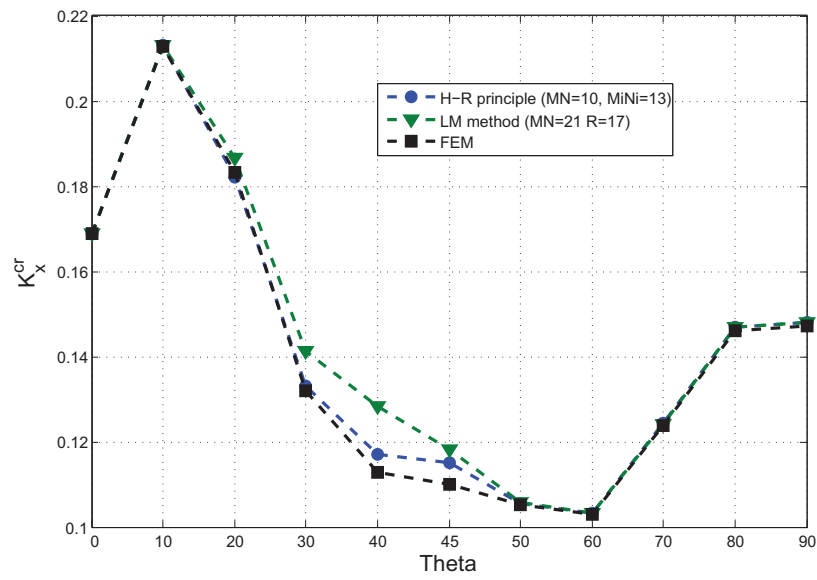


FIG. 11. Non-dimensional buckling coefficients varying with fibre angle for $[+\theta]_n$ SSSF long plate obtained by using the LM method and the H-R principle.